論文 / 著書情報
Article / Book Information

Title	Multi-Flame VAD Process for High-Rate Fabrication of Optical Fiber Preforms.
Authors	SHUICHI SHIBATA, Motohiro Nakahara
Citation	The transactions of the IECE OF Japan, Vol. E69, No. , pp. 1206-1212
Pub. date	1986, 11
URL	http://search.ieice.org/
Copyright	(c) 1986 Institute of Electronics, Information and Communication Engineers

THE TRANSACTIONS OF THE IECE OF JAPAN, VOL. E 69, NO. 11 NOVEMBER 1986

PAPER

Multi-Flame VAD Process for High-Rate Fabrication of Optical Fiber Preforms

Hiroyuki SUDA†, Shuichi SHIBATA† *and*
Motohiro NAKAHARA††, *Members*

SUMMARY A new burner with a multi-flame structure is proposed for high-rate fabrication of optical fiber preforms in the vapor-phase axial deposition process (VAD). In this multi-flame VAD process, the synthesis of fine glass particles was clarified and the fabrication of soot preforms was investigated together with the consolidation process. As a result, a deposition rate of 4.5 g/min was achieved using one double-flame burner. Graded-index core preform size was increased to 2500 g. In addition, fibers with a high numerical aperture (N. A.) of 0.28 were fabricated using a double-flame burner. A transmission loss at 1.62 μm was 0.54 dB/km and the bandwidth at 1.3 μm was 440 MHz km.

1. Introduction

In the field of optical fiber fabrication, much emphasis has been placed on modifying and scaling-up of processes to improve cost effectiveness and manufacturability. In particular, increasing the deposition rate for fiber preform synthesis has greatly contributed to reduced fiber cost and ease of mass production[1],[2]. Moreover, there have been rapid improvements in fiber drawing techniques, and today fiber drawing speed has increased significantly[3],[4]. Thus, larger preforms, of high N. A. fibers particularly, are in great demand for subscriber systems and data links. Because of the sheer volume of required fibers for subscriber systems and data links, it is absolutely essential that they be low-cost.

The authors previously reported on a high-rate deposition technique for the VAD process by optimizing the burner flame stream. A maximum preform deposition rate of 4.5 g/min was achieved using the two conventional single-flame burner process[5]. However, in the conventional burner process, as the raw material feed rate increased, the deposition yield decreased and soot preform growing tended to be unstable. The cause was thought to be due to the increase in the amount of non-reacted raw materials. A stable high-rate fabrication process with a high deposition yield has been demanded.

This paper presents the details of the multi-flame VAD process for stable high-rate preform fabrication and describes fabricating techniques using a double-flame burner for high N. A. optical fibers. In addition, the influence of preform size on consolidation conditions is also discussed to obtain a large transparent preform.

Manuscript received June 23, 1986.

†The authors are with NTT Electrical Communications Laboratories, 162, Ibaraki-ken, 319-11 Japan.

††The author is with NTT Research and Development Headquarters, Musashino-shi, 180 Japan.

2. Multi-Flame VAD Process

2.1 Outline of Multi-Flame VAD Process

The multi-flame VAD process is shown schematically in Fig. 1. The burner employed in this process has two or more flames, resulting in the double-flame structure shown in the figure. The outer flame originates from the top burner while the inner flame is spaced rearwardly and below the outer flame. Fine glass particles are generated from vaporized reagents in the inner flame and grow larger as they travel through the outer flame. These particles are deposited on the end of the soot preform. The soot preform, growing in an axial direction, is pulled upward.

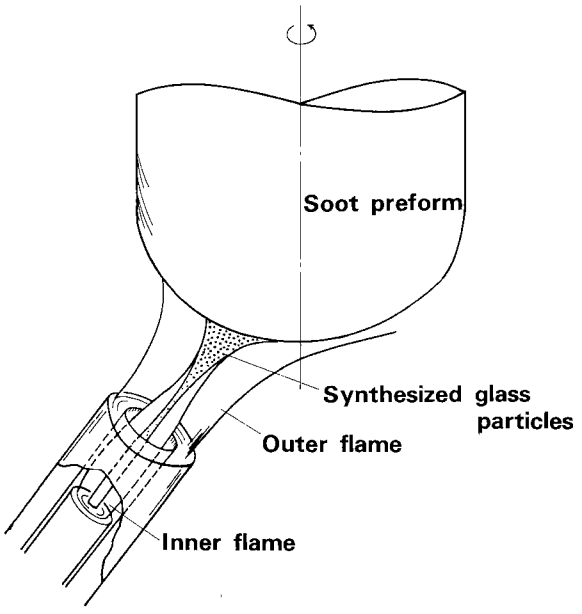

Fig. 1 Schematic illustration of multi-flame VAD process.

2.2 Multi-Flame VAD Burner Design

The specific surface area of synthesized fine glass particles at different flow speeds of raw material gas in the flame were measured by B. E. T. method. The size of the fine glass particles is plotted against the time required to pass through the flame region in Fig. 2. Particle size increases as the pass-through time increases. It is found that synthesized particle size is controlled by regulating pass-through time. The pass-through time can be regulated by varying the flow speed of raw material gas or by changing the flame length.

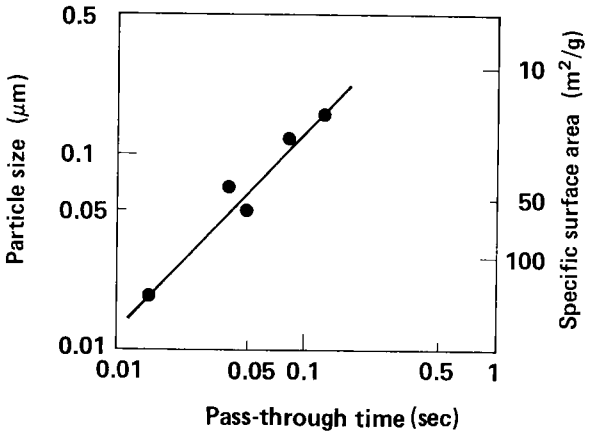

Fig. 2 Relationship between synthesized particle size and pass-through time.

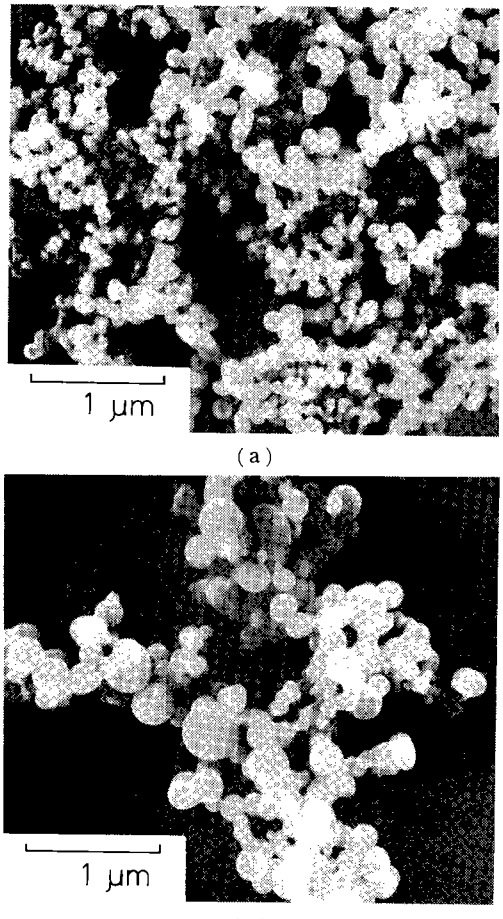

Fig. 3 SEM photographs of glass particles synthesized by (a) inner flame only and (b) double-flame.

The multi-flame VAD burner is designed so that the flame length is extended by the displacing the inner flame orifice rearwardly relative to the outer flame orifice, such as the double-flame burner with two flames shown in Fig. 1. Consequently, the time available for the reaction increases and the synthesized particles increase in size. SEM photographs of fine glass particles synthesized by inner flame only, i.e. conventional single flame, and also by double-flame are shown in Figs. 3(a) and 3(b). Glass particles synthesized by a double-flame burner have a maximum diameter of 0.5 μm, while those synthesized by inner flame are only 0.1 μm in diameter.

2.3 Deposition Characteristics Using a Double-Flame Burner

The particle deposition rate was measured in the following experiment. A silica glass quasi-preform was prepared as a deposition target. The oxy-hydrogen flame composition was held constant and the weight of deposited glass particles was measured for different $SiCl_4$ feed rates. The deposition rate is given as a function of the $SiCl_4$ feed rate in Fig. 4. The solid line represents the deposition rate under double-flame conditions and the dashed line represents the data under inner flame only conditions. The deposition rate under the

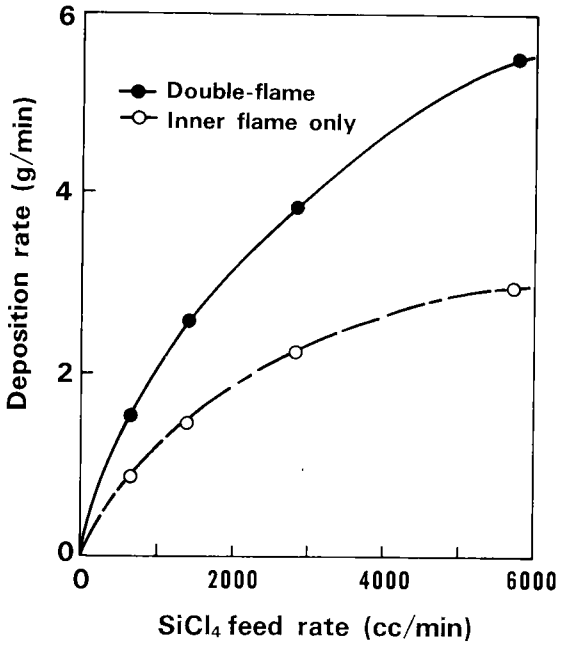

Fig. 4 Particle deposition characteristics using double-flame burner.

double-flame condition was about 1.5 times larger than that for the inner flame only. It was observed that an increase at a large raw material feed rate was greater than that at a small feed rate. The multi-flame structure is more effective for synthesizing soot preforms at large raw material feed rates.

3. Soot Preform Fabrication Using a Double-Flame Burner

3.1 Soot Preform Synthesizing

Fabrication of large core soot preforms with a graded-index profile was carried out using a double-flame VAD burner. Fabrication parameters were chosen by taking the flame length extention and high reactivity into consideration. A high deposition rate of 3.5~4.5 g/min/burner and high fabrication stability were obtained, resulting in the large and long core soot preform shown in Fig. 5(a). The consolidated transparent preform is shown in Fig. 5(b). The outer diameter was 130 mm and the soot preform length was 900 mm. The consolidated preform weighed 2500 g, had an outer diameter of 55 mm and a length of 500 mm. From this preform it was possible to draw 580 km of fiber with a core diameter of 50 μm. The overall deposition yield was greater than 55 %. The consolidation process is described in Chap. 4.

3.2 Characteristics of GeO_2 Doping

The feed rate of $GeCl_4$ was increased and then core preforms having different GeO_2 concentrations were synthesized using a double-flame VAD burner. The other fabrication parameters, such as $SiCl_4$ feed rate and oxygen and hydrogen gas flow rates, were held constant for each preform fabrication. Deposition rates for soot preforms were 3.4~3.8 g/min.

Figure 6 shows the relationship between the relative refractive index difference Δ, for the transparent preforms and the $GeCl_4$ concentration in the raw material gas flow. A $GeCl_4$ concentration of 18 mol % produced a relative refractive index difference of 2.0 %.

3.3 Refractive Index Profile Control

It is necessary to precisely control the refractive index profile for the graded-index fiber preform fabrication. In the conventional VAD process, the surface temperature distribution during soot preform synthesis plays a major role in determining the refractive index profile[6]. Although both conventional and multi-flame VAD processes are fundamentally the same, controlling the refractive index profile in the multi-flame VAD process is more complex than in the conventional proc-

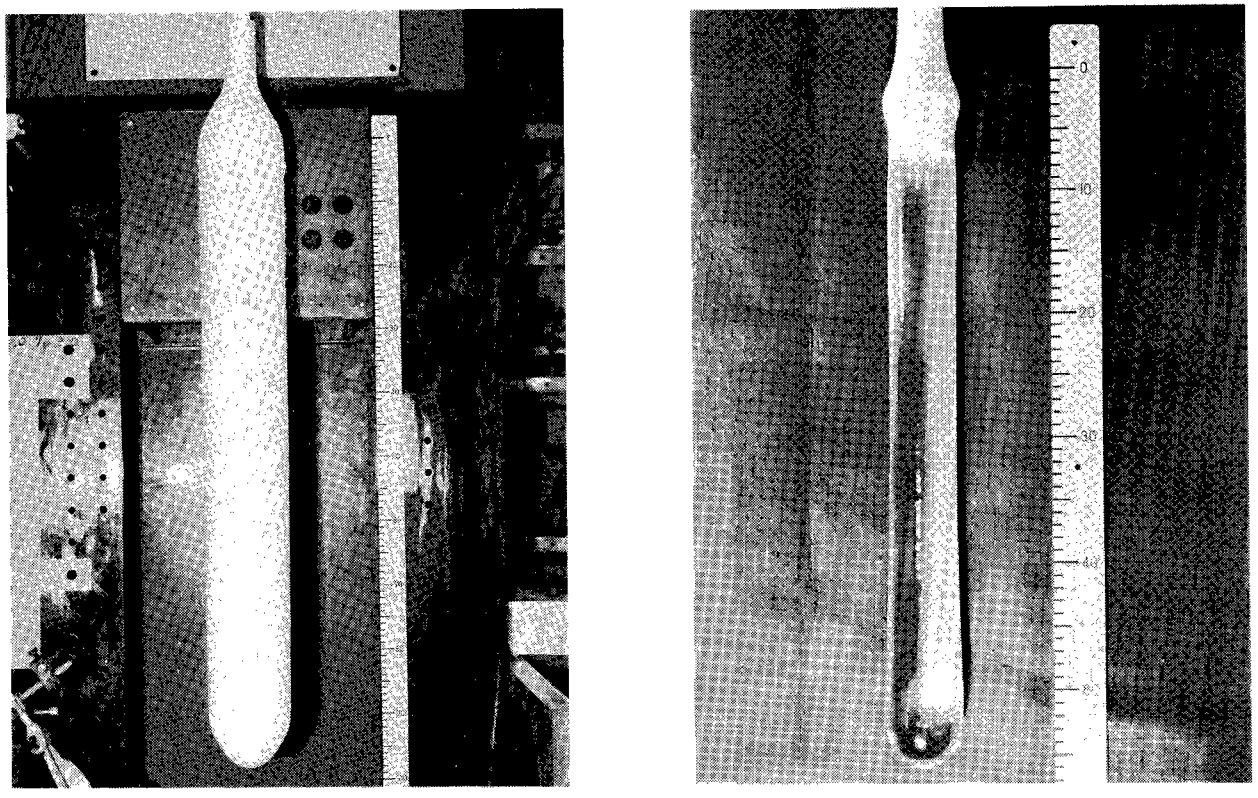

(a) (b)

Fig. 5 High-rate deposited large preform; (a) soot preform and (b) consolidated transparent preform.

ess because of its complex flame structure.

Using the double-flame burner, an appropriate surface temperature distribution was attained on the soot preform by choosing the correct ratio between the hydrogen gas flow rates of the inner and outer flames.

The refractive index profile obtained with a high relative refractive index difference of 1.8 % is shown in Fig. 7. The refractive index profile was measured by a spatial filtering technique using a standard of silica glass. A parabolic refractive index profile was also formed using the double-flame VAD burner.

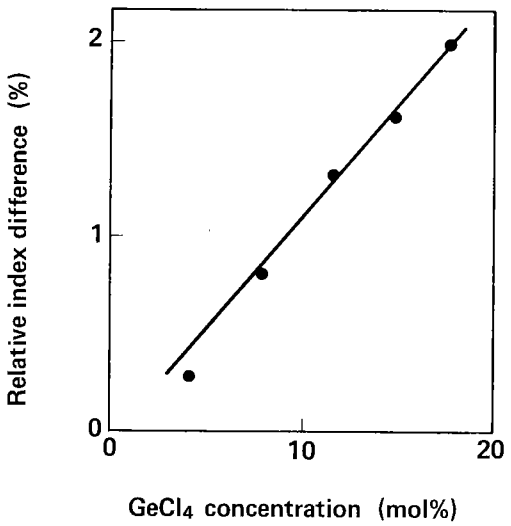

Fig. 6 Relationship between $GeCl_4$ concentration in raw material gas flow and relative refractive index difference for consolidated preforms.

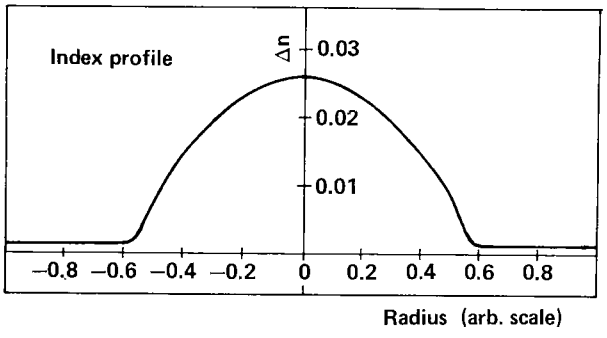

Fig. 7 Refractive index profile for high-rate deposited preform with high relative refractive index difference of 1.8 %.

4. Consolidation Process

4.1 Consolidation Conditions for Large Soot Preforms

Soot preforms fabricated by the multi-flame VAD process were large in diameter. Some clouds remained in large preforms consolidated under the same condition for conventional VAD soot preforms. Moreover, preforms with high GeO_2 concentration intended to be more cloudy than those with low GeO_2 concentration.

Therefore, an accurate experiment was conducted to determine consolidation conditions for large soot preforms. A large soot preform, 130 mm in diameter, was sectioned into three 80 mm thick parts.

Each sample was consolidated under different conditions and these are given in Table 1, where T_0 is the standard furnace temperature (i.e. 1550°C) and C_0 is the standard temperature increase rate (i.e. 10 °C/min). The consolidated samples were polished and their absorption coefficients measured. The results are shown in Fig. 8. For large preform consolidation, two key points were found, a high furnace temperature and slow temperature increase.

In general, the critical pore diameter d_c under various consolidation condition can be given by

$$d_c = k_1 + \sqrt{k_2 + k_3 \frac{SDT^2}{C}} \qquad (1)$$

where S and D are the solubility and the diffusion coefficient of ambient gas, T is the furnace temperature, C is the temperature increase rate and $k_{1,2,3}$ are constants[7]. As the critical diameter is larger, it is easier to consolidate soot preforms completely. This equation can qualitatively explain the results in the present experi-

Table 1 List of consolidation conditions.

Sample number	Furnace temperature (°C)	Temperature increase rate (°C/hr)
1	T_0	C_0
2	T_0 + 100	C_0
3	T_0 + 50	C_0 / 3

T_0 : Standard furnace temperature
C_0 : Standard temperature increase rate

ment. However, this representation is not sufficient to explain that large soot preforms can not be completely consolidated under the same conditions. Thus, another factor must be taken into consideration.

4.2 Influence of Soot Preform Diameter

The results above suggest that soot preform size cause the optimal conditions to change and also that heat transfer should be taken into consideration. Thus, shrinkage in the transient state was examined using the following model.

It is assumed that a soot preform is infinitely long and the heat is constantly supplied. The thermal conduction equation with respect to time t and radial position r, which takes both the initial and boundary conditions into account, is given by

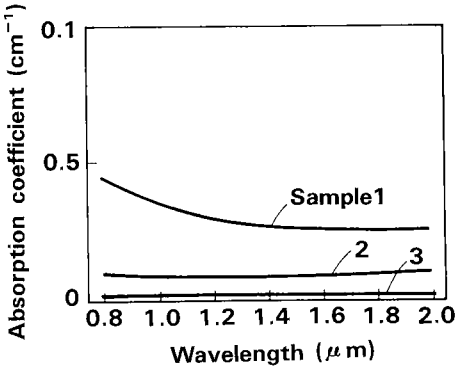

Fig. 8 Absorption coefficients of consolidated preforms under different consolidation conditions.

$$\frac{\partial T}{\partial t}=\chi^2\left(\frac{\partial^2 T}{\partial r^2}+\frac{1}{r}\frac{\partial T}{\partial r}\right) \tag{2}$$

$$\left.\begin{aligned} &T=0,\ q_0=0 \quad \text{when } t=0\\ &K\frac{\partial T}{\partial r}=q_0 \quad \text{when } r=a\\ &\frac{\partial T}{\partial r}=0 \quad \text{when } r=0 \end{aligned}\right\} \tag{3}$$

where T is the temperature, χ^2 is the thermometric conductivity ($=K/c\rho$; K is the thermal conductivity, c is the specific heat capacity and ρ is the density), q_0 is the supplied heat flux and a is the soot preform diameter [8].

The above thermal conduction equation is satisfied by the solution, as follows

$$T=\frac{2q_0}{aK}\left[\chi^2 t+\frac{r^2}{4}-\frac{a^2}{8}-a^2\sum_{n=1}^{\infty}\frac{J_0(\alpha_n r/a)}{\alpha_n^2 J_0(\alpha_n)}\right.$$
$$\left.\times\exp\{-(\chi\alpha_n/a)^2 t\}\right] \tag{4}$$

where $J_0(x)$ is the Bessel function of order zero of the first kind and α_n, $n=1,2,\cdots$ are the positive roots of $J_1(\alpha)=0$.

Rough assumptions are employed, thermal conductivity is constant and soot preforms have homogeneous initial apparent density. The viscosity coefficient and shrinkage data are taken from Scherer's reports[9],[10] so the temperature at each divided cell can be calculated when time t has passed, and linear shrinkage can be estimated by taking the sum of a series of sequential steps as shown in Fig. 9.

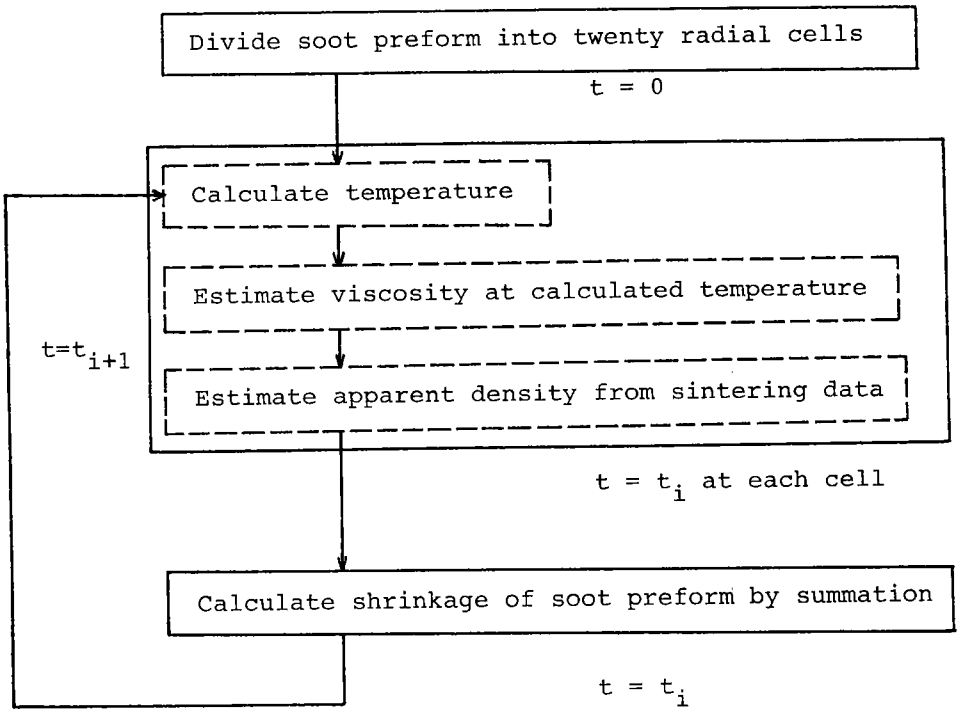

Fig. 9 Calculation steps for linear shrinkage of soot preform.

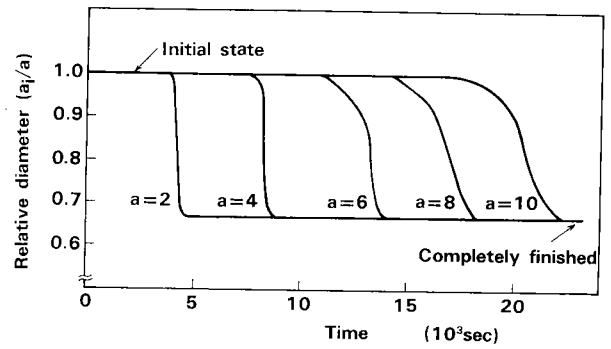

Fig. 10 Shrinkage of soot preforms with different outer diameter, where a is the initial soot preform diameter.

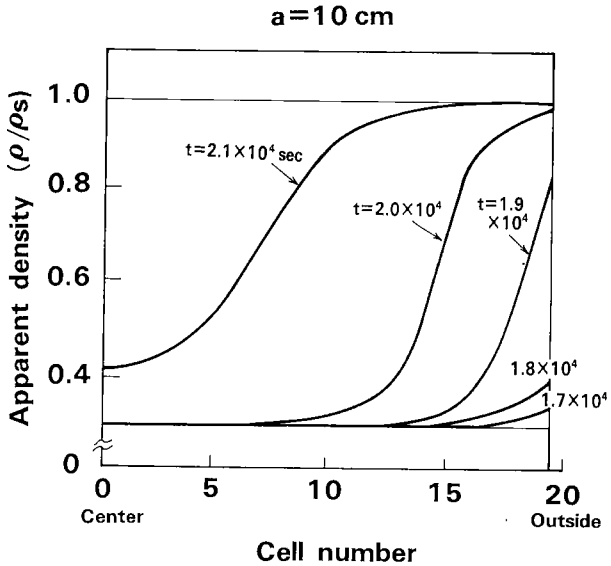

Fig. 11 Shrinkage distribution for soot preform, where ρ is the apparent density and ρ_s is the true density (=2.2 g/cm^3 for silica glass).

The shrinking process in soot preforms with different diameters is shown in Fig. 10. More time is required to completely consolidate the soot preform as the diameter of that increases. Shrinkage time was roughly proportional to the soot preform diameter. The apparent density distribution in the soot preform at different passing times is given in Fig. 11. Shrinkage was delayed at the preform center. It is anticipated that the temperature increase rate becomes fast as it is inward. Consequently, the consolidation conditions for large soot preforms become severe. The influence of soot preform diameter on the consolidation is thought to be enhanced for high GeO_2 doped preforms because ambient gas constants, such as the solubility and diffusion coefficient, lessen due to the GeO_2 becoming volatile.

5. Fiber Characteristics

Fibers with a 125 μm outer diameter, were drawn from preforms fabricated using the double-flame burner.

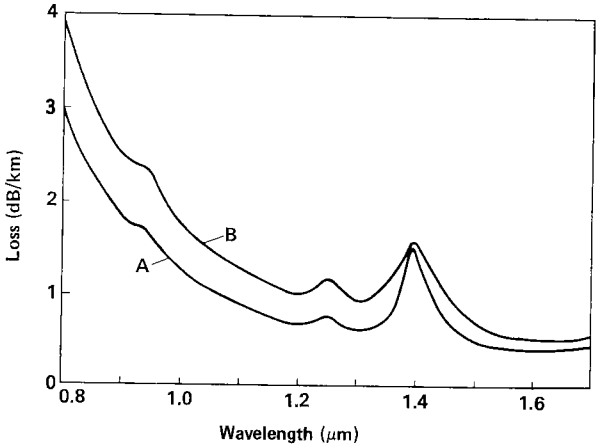

Fig. 12 Transmission loss spectra for high-rate deposited fibers with relative index differences of (A) 1.0 % and (B) 1.8 %.

Figure 12 shows transmission loss spectra for fabricated fibers with a relative refractive index difference of 1.0 % and 1.8 %, designated by A and B. The minimum loss of A was 0.44 dB/km at 1.55 μm and B, 0.54 dB/km at 1.62 μm. Transmission bandwidth for the high N.A. fiber B was 440 MHz km at 1.3 μm.

It was confirmed that fibers fabricated using the multi-flame VAD process had good transmission characteristics.

6. Conclusion

A multi-flame VAD process was proposed and developed for high-rate fabrication of optical fiber preforms. A high deposition rate of 4.5 g/min was attained and large preforms were stably fabricated. It was clarified that a high furnace temperature and a slow temperature increase were necessary for large soot preform consolidation. Fibers drawn from the high-rate deposited preforms exhibited low transmission loss and wide transmission bandwidth.

Using the multi-flame VAD process, it is possible to mass-produce optical fiber preforms and thereby reduce the cost of manufacturing optical fibers.

Acknowledgements

The authors would like to thank Hisao Takata, Nobuo Inagaki, Shinzoh Yamakawa and Masaharu Horiguchi for their many thoughtful suggestions. Thanks are also due to Sumiko Itoh for making the fiber loss measurements used in this study and to Takeshi Kinoshita for his helpful assistance with the consolidation experiment.

References

(1) K. L. Walker, F. T. Geyling and S. R. Nagel: "Thermophoretic deposition of small particles in modified chemical

vapor deposition process", J. Am. Ceram. Soc., **63**, p. 552 (1980).
(2) M. G. Blankenship, A. J. Morrow and L. A. Silverman : "Large GRIN preforms deposited at high rate using OVD", Tech. Dig. Conf. Opt. Fiber Commun., p. 18, Phoenix (1982).
(3) U. C. Peak and C. M. Schroeder : "Optical fibers coated with a UV-curable material at a speed of 12 m/s", Electron. Lett., **20**, p. 304 (1984).
(4) S. Sakaguchi and T. Kimura : "A 1200 m/min speed drawing of optical fibers with pressurized coating", Tech. Dig. Conf. Opt. Fiber Commun., p. 18, San Diego (1985).
(5) H. Suda, S. Sudo and M. Nakahara : "Fine glass particle-deposition mechanism in the VAD process", Fiber & Integrated Opt., **4**, p. 427 (1983).
(6) S. Sudo, M. Kawachi, H. Suda, M. Nakahara and T. Edahiro : "Refractive-index profile control techniques in the vapor-phase axial deposition method", Trans. IECE Japan (Section E), **E64**, pp. 536-543 (Aug. 1981).
(7) S. Sudo, T. Edahiro and M. Kawachi : "Sintering process of porous preforms made by a VAD method for optical fiber fabrication", Trans. IECE Japan (Section E), **E63**, 10, pp. 731-737 (Oct. 1980).
(8) H. S. Carslow and J. C. Jaeger : "Conduction of heat in solids", 2 nd. ed., Oxford Univ. Press (1959).
(9) G. W. Scherer : "Sintering of low-density glasses, I : Theory", J. Am. Ceram. Soc., **60**, p. 236 (1977).
(10) G. W. Scherer and D. L. Bachman : "Sintering of low-density glasses, II : Experiment study", J. Am. Ceram. Soc., **60**, p. 239 (1977).

Hiroyuki Suda received the B.E. and M.E. degrees in instrumentation engineering from Keio University, Yokohama, Japan, in 1976 and 1978, respectively. He joined the NTT Electrical Communications Laboratories in 1978 and has been engaged in research and development for VAD optical fiber fabrication.
Mr. Suda is a member of the Japan Society of Applied Physics and the Ceramic Society of Japan.

Shuichi Shibata received the B.S. and M.S. degrees from Hokkaido University in 1970 and 1973, respectively. In 1983, he received the Dr. E. degree in the area of fiber glasses for optical communication.
Since 1973, he has been engaged in the research and development of the various optical fibers: multicomponent glass fibers, infrared-transmitting optical fibers and VAD fibers, etc., in the NTT Electrical Communications Laboratories.
Dr. Shibata is a member of the Japan Society of Applied Physics.

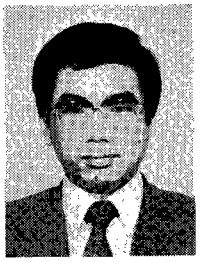

Motohiro Nakahara received the B.S., M.S., and Ph.D. degrees in physics from Kyushu University in 1966, 1969 and 1977, respectively. Since 1969, He had worked at the NTT Electrical Communications Laboratories on oxide single crystal and VAD fiber fabrication method. He is presently a senior manager in NTT Research and Development Headquarters.
Dr. Nakahara is a member of the Japan Society of Applied Physics. He received the Achievement Award from IECE of Japan in 1981 for his work on the VAD method for fiber fabrication.